Monitoring of Gefitinib Sensitivity with Radioiodinated PHY Based on EGFR Expression

Mitsuyoshi Yoshimoto,*[a,b] Masahiko Hirata,[c] Yasukazu Kanai,[d] Sadahiro Naka,[e] Ryuichi Nishii,[f] Shinya Kagawa,[g] Keiichi Kawai,[b] and Yoshiro Ohmomo[c]

[a] *Division of Functional Imaging, National Cancer Center Hospital East; 6–5–1 Kashiwanoha, Kashiwa, Chiba 277–8577, Japan:* [b] *Faculty of Health Sciences, Kanazawa University; 5–11–80 Kodatsuno, Kanazawa, Ishikawa 920–0942, Japan:* [c] *Osaka University of Pharmaceutical Sciences; 4–20–1 Nasahara, Takatsuki, Osaka 569–1094, Japan:* [d] *Department of Molecular Imaging in Medicine, Osaka University Graduate School of Medicine;* [e] *Department of Nuclear Medicine and Tracer Kinetics, Osaka University Graduate School of Medicine; 2–2 Yamadaoka, Suita, Osaka 565–0871, Japan:* [f] *Department of Radiology, Faculty of Medicine, University of Miyazaki; 5200 Kihara, Kiyotake-cho, Miyazaki 889–1692, Japan: and* [g] *Research Institute, Shiga Medical Center; S 5–4–30 Moriyama, Moriyama, Shiga 524–8524, Japan.*

Received July 16, 2013; accepted December 10, 2013

Epidermal growth factor receptor (EGFR) is attractive target for tumor diagnosis and therapy, as it is specifically and abundantly expressed in tumor cells. EGFR-tyrosine kinase (TK) inhibitors such as gefitinib and erlotinib are widely used in the treatment of non-small cell lung cancer (NSCLC). In this study, we investigated whether radioiodinated 4-(3-iodo-phenoxy)-6,7-diethoxy-quinazoline (PHY), which is a candidate EGFR-TK imaging agent for single photon emission computed tomography (SPECT) is able to predict gefitinib sensitivity. We used four NSCLC cell lines-A549 (wild-type EGFR), H1650 (mutant EGFR; del E746_A750), H1975 (mutant EGFR; L858R, T790M) and H3255 (mutant EGFR; L858R)-and one epidermoid carcinoma cell line, A431 (wild-type EGFR). Cell proliferation assay and Western blotting revealed that A431 and H3255 with high EGFR expression showed high sensitivity to gefitinib. On the other hand, A549, H1650 and H1975 showed much lower sensitivity to gefitinib. The blocking study revealed that gefitinib decreased tumor uptake in ^{125}I-PHY in A431-bearing mice. Moreover, *in vivo* tumor uptake of ^{125}I-PHY was correlated with the IC_{50} of gefitinib for cell proliferation. In the present study, tumor uptake of ^{125}I-PHY was correlated with the gefitinib sensitivity and this uptake was based on expression levels of EGFR, but not on mutation status. Although the mutation status is the most important factor for predicting gefitinib sensitivity, the abundant expression of EGFR is essential for therapy with EGFR-TK inhibitors. Therefore, radioiodinated PHY is a potential imaging agent to predict gefitinib sensitivity based on EGFR expression levels though further modifications of the imaging agent is needed to accurately estimate the mutation status.

Key words tumor imaging; gefitinib; epidermal growth factor receptor tyrosine kinase; lung cancer; single photon emission computed tomography

Epidermal growth factor receptor (EGFR) is overexpressed in a variety of tumors including non-small cell lung cancer (NSCLC), head and neck cancer, glioma and ovarian cancer.[1,2] Activation of EGFR tyrosine kinase (EGFR-TK) is involved in the proliferation, invasion, metastasis, angiogenesis and suppression of apoptosis.[3] Therefore, EGFR is an attractive target molecule for tumor diagnosis and therapy.

To date, numerous EGFR-TK inhibitors and anti-EGFR antibodies have been developed and used in clinical settings.[2,4] Gefitinib, an EGFR-TK inhibitor, has been approved as a molecular targeted agent for the treatment of advanced NSCLC. Gefitinib leads to rapid symptom improvement and tumor regression in patients with NSCLC. Tumor responses were, however, observed in only 10–19% of patients with NSCLC in the phase II trial.[5,6] In addition, interstitial lung disease is a serious and fatal adverse effect of gefitinib treatment.[7] Retrospective epidemiologic analyses have revealed that the therapeutic effects are more apparent in Japanese, women and non-smokers.[8] From recent molecular biological studies,[9–11] mutations in the TK domain of EGFR gene are closely associated with gefitinib sensitivity. Therefore, development of diagnostic technology is necessary to predict or estimate therapeutic efficacy by EGFR-TK inhibitors.

Nuclear medicine techniques (positron emission tomography; PET and single photon emission computed tomography; SPECT) are able to estimate physiological and biological functions at the molecular or gene levels, as well as pharmacokinetics *in vivo*.[12,13] Radiolabeled inhibitors are believed to clarify pharmacokinetics, expression levels and functions of target molecules, and to estimate the therapeutic efficacy of the inhibitors. Although ^{18}F-gefitinib was investigated to monitor EGFR expression and mutation status, tumor uptake was not correlated with EGFR expression levels and mutation status.[14] Development of various EGFR-TK imaging agents based exclusively on the anilinoquinazoline structure has been attempted for more than a decade, but further optimization of the properties of imaging agents with respect to high specificity to EGFR, selectivity to mutant types of kinase and high tumor uptake is required.[15–20] Thus, novel imaging agents to accurately detect EGFR-TK activity are needed in order to predict and monitor the therapeutic effects.

We have reported that radioiodinated 4-(3-iodo-phenoxy)-6,7-diethoxy-quinazoline (PHY, Fig. 1) is a candidate EGFR-TK imaging agent for SPECT.[21] In this report, we measured the uptake of ^{125}I-PHY in tumors with various expression levels of EGFR and types of mutation, and investigated whether gefitinib sensitivity can be estimated with radioiodinated PHY.

The authors declare no conflict of interest.

* To whom correspondence should be addressed. e-mail: miyoshim@ncc.go.jp

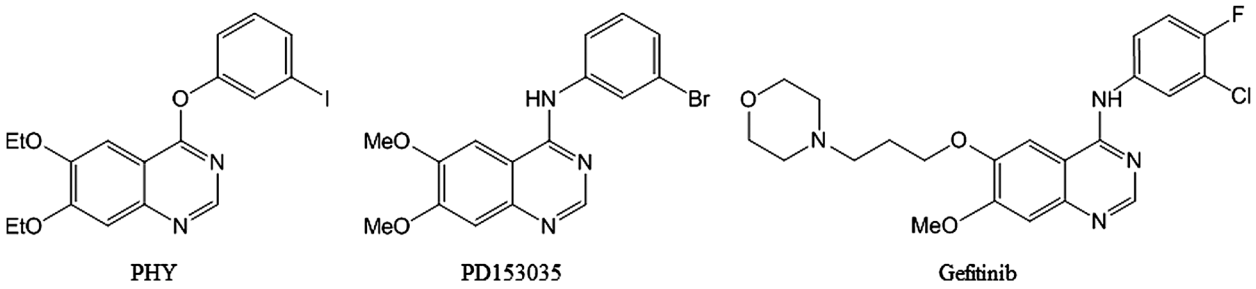

Fig. 1. Chemical Structures of 4-(3-Iodo-phenoxy)-6,7-diethoxy-quinazoline (PHY), PD153035 and Gefitinib

Table 1. Characterization and Sensitivity to Gefitinib in Tumor Cell Lines Used in This Study

Cell lines	Origin	EGFR status	IC_{50} (μM)
A431	Human epidermoid carcinoma	Wild-type	1.8
A549	Human NSCLC (Adenocarcinoma)	Wild-type	17.4
H1650	Human NSCLC (Adenocarcinoma)	del E746-A750	12.1
H1975	Human NSCLC (Adenocarcinoma)	L858R, T790M	13.3
H3255	Human NSCLC (Adenocarcinoma)	L858R	0.02

MATERIALS AND METHODS

Cell Culture Four NSCLC cell lines-A549 (wild-type EGFR), H1650 (mutant EGFR; del E746_A750), H1975 (mutant EGFR; L858R, T790M) and H3255 (mutant EGFR; L858R)-and one epidermoid carcinoma cell line, A431 (wild-type EGFR), were used in this study (Table 1). A431 and A549 were obtained from DS Pharma Biomedical (Osaka, Japan). H1650 and H1975 were purchased from the American Tissue Culture Collection (Manassas, VA , U.S.A.). H3255 was kindly provided by Dr. Juri Gelovani (M.D. Anderson Cancer Center). A431 and A549 were maintained in Dulbecco's modified Eagle's medium (DMEM; Sigma, St. Louis, MO, U.S.A.) supplemented with 10% fetal bovine serum (FBS; Invitrogen Inc., Carlsbad, CA, U.S.A.). H1650 and H1975 were maintained in RPMI1640 (Sigma) supplemented with 10% FBS and 2 mM glutamine. H3255 was maintained in DMEM/F12 (Sigma) supplemented with 20% FBS. All cells were cultured in a 5% CO_2-humidified atmosphere at 37°C.

Growth Inhibition Assay Growth inhibition by gefitinib was assessed using CellTiter 96® AQ_{ueous} One Solution Cell Proliferation Assay Kit (Promega, Madison, WI, U.S.A.). Cells were seeded in 96-well plates and incubated in culture media overnight at 37°C. The numbers of cells per well used in these experiments were as follows: 4000 for A431; 1000 for A549; 3000 for H1650; 2500 for H1975; and 5000 for H3255. After incubation with gefitinib, PD153035 and PHY at concentrations ranging from 1 nM to 33.3 μM for 72 h, 20 μL of CellTiter 96® AQ_{ueous} One Solution was added to each well and plates were incubated for a further 2 h at 37°C. Absorbance was measured at 490 nm using a micro-plate reader. Each experiment was set up in four replicate wells for each drug concentration and was repeated at least 4 times. IC_{50} values were determined using a nonlinear regression model with a sigmoidal dose response (GraphPad Prism version 4.00 for Widows; GraphPad Software, San Diego, CA, U.S.A.).

Western Blotting Cells were lysed in radio immunoprecipitation assay (RIPA) buffer [50 mM Tris–HCl (pH 8.0), 150 mM NaCl, 1% NP-40, 0.5% deoxycholic acid sodium salt, 0.1% sodium dodecyl sulfate (SDS)] containing protease inhibitor cocktail (Nacalai Tesque, Kyoto, Japan) and phosphatase inhibitor cocktail (Nacalai Tesque). Protein concentration was determined using BCA Protein Assay Reagent kit (Thermo-Fisher Scientific, Rockford, IL, U.S.A.). Lysates were separated by SDS-polyacrylamide gel electrophoresis (PAGE) and transferred onto a polyvinylidene difluoride (PVDF) membrane (Immobilon-FL, Millipore, Billerica, MA, U.S.A.). Membranes were blocked for 1 h in LI-COR blocking buffer and were incubated with primary and secondary antibodies. Rabbit polyclonal anti-EGFR (SC-03) (Santa Cruz Biotechnology, Santa Cruz, CA, U.S.A.), anti-phospho-EGFR (Tyr1068) (Cell Signaling Technology, Danvers, MA, U.S.A.) and mouse monoclonal anti-β actin (Sigma) were used as primary antibodies. Alexa Fluor 680 goat anti-rabbit immunoglobulin G (IgG) (Molecular Probes, Eugene, OR, U.S.A.) and IRDye 800 anti-mouse IgG (Rockland Immunochemicals, Gilbertsville, PA, U.S.A.) were used as secondary antibodies. Membranes were scanned and bands were detected using the Odyssey Infrared Imaging System (LI-COR Biosciences, Lincoln, NE, U.S.A.).

Tumor Xenograft Model Animal studies were performed in compliance with the guidelines for the care and use of laboratory animals of Kanazawa University. Biodistribution studies were conducted in nude mice bearing tumors. Female BALB/c nu/nu mice aged 5–6 weeks (Japan SLC, Inc. Hamamatsu, Japan) were xenografted s.c. in the right and left dorsum with $2–5\times10^6$ cells. Tumor size was below 1 cm in diameter.

Radiosynthesis of ^{125}I-PHY ^{125}I-NaI (MP Biomedicals, Santa Ana, CA, U.S.A.) and 10 μL of 0.1 N HCl were added to 20 μL of tributylstannyl precursor (1 mg/mL in EtOH), followed by addition of 10 μL of 30% hydrogen peroxide. After mixing for 5 min, the reaction was quenched by adding 10 μL of 10% sodium metabisulfate. Purification of ^{125}I-PHY was performed by HPLC using a Cosmosil $5C_{18}$-AR II column (10×250 mm; Nacalai Tesque) eluted with 85% MeOH and 15% water at a flow rate of 2.0 mL/min.

Biodistribution of ^{125}I-PHY in Tumor-Bearing Mice

Tumor-bearing mice were injected *via* the tail vein with 74 kBq/100 μL (saline) of ^{125}I-PHY. Mice were sacrificed at 1, 4 and 24 h post-injection, and tissue samples were excised. To investigate EGFR-TK-specific uptake of ^{125}I-PHY, gefitinib (10 mg/kg) was co-injected with ^{125}I-PHY. Biodistribution was determined at 4 h post-injection. Tissue samples were weighed and radioactivity was measured with a γ-counter (ARC-360, Aloka, Tokyo, Japan). Uptake in organs was expressed as the percentage of injected dose per gram of tissue (%ID/g).

Statistical Analysis Data analysis was performed using GraphPad Prism. Unpaired *t*-test was used for the blocking study. The correlation between IC_{50} of gefitinib and tumor uptake of ^{125}I-PHY was tested using Spearman correlation test. The results were considered statistically significant at $p<0.05$.

RESULTS

Expression of EGFR and Phospho-EGFR and Growth Inhibition by Gefitinib We used five tumor cell lines (2 wild-type EGFR and 3 mutant EGFR) and analyzed EGFR and phosphorylated EGFR (phospho-EGFR) expression levels by western blotting (Fig. 2). IC_{50} values for growth inhibition by gefitinib were also measured by MTS assay (Table 1). There was high expression of EGFR and phospho-EGFR in A431 and H3255, whereas the IC_{50} of H3255 (L858R) (0.02 μM) was much lower than that of A431 (1.8 μM). The highest IC_{50} was observed in A549 (17.4 μM), although the expression of EGFR and phospho-EGFR was moderate. H1650 (del E746-A750) and H1975 (L858R+T790M) showed lower expression of EGFR and phospho-EGFR, and the IC_{50} values for H1650 and H1975 were 12.1 μM and 13.3 μM, respectively.

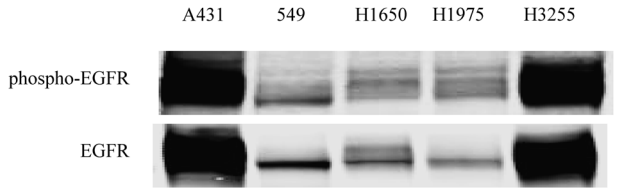

Fig. 2. Expression of EGFR and Phospho-EGFR, as Detected by Western Blotting

Effect of L858R Mutation on Growth Inhibition by EGFR Inhibitors In order to investigate whether EGFR mutations affect growth inhibition by PHY and gefitinib, A431 and H3255 were selected because they have abundant expression of EGFR and show different gefitinib sensitivity. The IC_{50} of PD153035, which is an analogue of PHY, was also measured to investigate the structure–activity relationship. All

Table 2. IC_{50} of Gefitinib, PD153035 and PHY against Cell Growth in A431 (Wild EGFR) and H3255 (L858R)

	A431	H3255	A431/H3255
Gefitinib (μM)	1.80	0.02	90.0
PD153035 (μM)	1.63	0.29	5.6
PHY (μM)	6.50	2.10	3.1

Table 3. Biodistribution of ^{125}I-PHY in A431-Bearing Nude Mice (n=4)

	1 h	4 h	24 h
Blood	0.72±0.06	0.62±0.09	0.03±0.01
Brain	0.24±0.02	0.06±0.01	0.00±0.00
Liver	3.30±1.15	1.62±0.78	0.07±0.02
Heart	0.65±0.10	0.27±0.04	0.02±0.01
Lung	1.08±0.17	0.51±0.04	0.06±0.04
Stomach	4.60±1.82	2.90±1.64	0.13±0.08
Kidney	1.33±0.16	0.62±0.06	0.03±0.01
Pancreas	0.84±0.13	0.31±0.07	0.01±0.01
Spleen	0.52±0.10	0.22±0.04	0.02±0.02
Muscle	1.12±0.39	0.23±0.01	0.05±0.06
Thyroid (%ID)	0.27±0.08	0.68±0.13	0.82±0.13
Intestine	30.57±6.07	22.70±5.14	0.92±0.55
A431	1.56±0.25	0.47±0.12	0.03±0.01

Data are expressed as %ID/g (mean±S.D.).

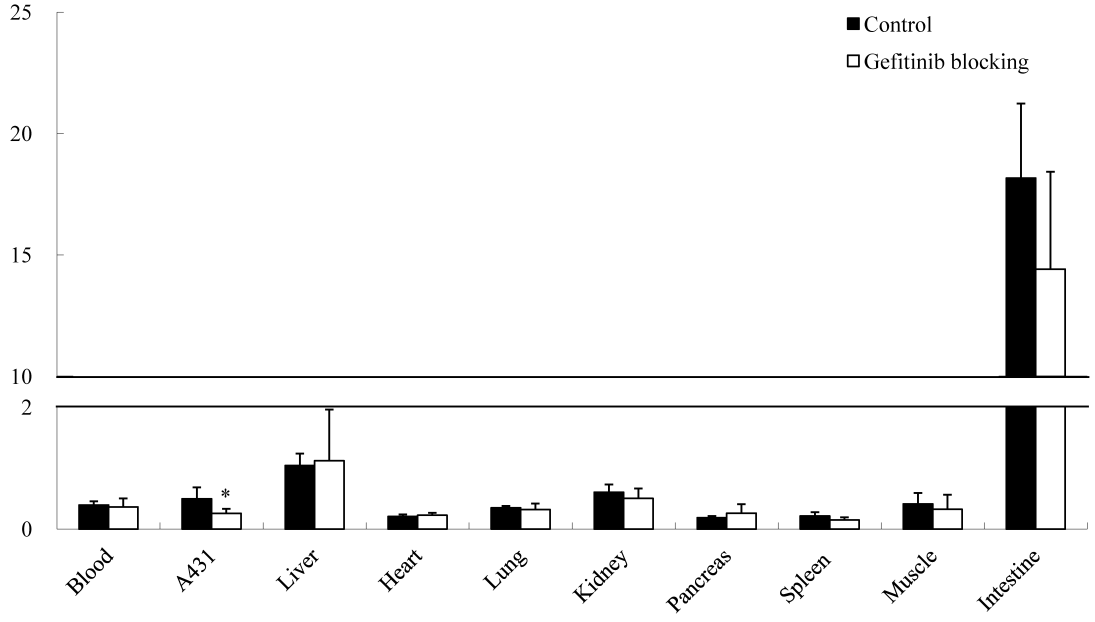

Fig. 3. Biodistribution of ^{125}I-PHY at 4 h with and without Co-injection of Gefitinib (n=3–4)

Radioactivity in tissues is expressed as %ID/g (mean±S.D.). *$p<0.05$ *vs.* control.

compounds showed potent growth inhibition in H3255 (Table 2). Increased inhibitory effects due to this mutation were only observed in gefitinib treatment. The IC_{50} in H3255 was more than 90-fold lower than that in A431, while the IC_{50} values for PD153035 and PHY in H3255 were only 5.6- and 3.1-fold lower than those in A431.

Biodistribution of ^{125}I-PHY in A431-Bearing Mice Table 3 shows the biodistribution of ^{125}I-PHY in A431-bearing mice. ^{125}I-PHY showed significant uptake in the intestine (30.6%ID/g at 1 h) and moderate uptake in the liver and stomach (3.3%ID/g and 4.6%ID/g at 1 h, respectively). There was low uptake of ^{125}I-PHY in other normal tissues. ^{125}I-PHY was rapidly cleared, whereas only the uptake in thyroid slowly increased up to 24 h post-injection (0.27%ID at 1 h to 0.82%ID at 24 h). Figure 3 indicates the effects of gefitinib on ^{125}I-PHY uptake at 4 h post-injection. Co-injection of gefitinib with ^{125}I-PHY resulted in a significant decrease in uptake in A431 (0.50%ID/g for control and 0.26%ID/g for gefitinib blocking).

Relationship between Tumor Uptake of ^{125}I-PHY and Gefitinib Sensitivity ^{125}I-PHY accumulated at various levels in tumors with different EGFR expression levels, as shown in Fig. 4 (1.56%ID/g for A431, 1.04%ID/g for A549, 1.31%ID/g for H1650, 0.94%ID/g for H1975 and 2.04%ID/g for H3255). Tumor uptake was reduced to less than half at 4 h post-injection. Tumors to blood (T/B) ratio and tumor to muscle (T/M) ratios were entirely good at 1 h post-injection (Fig. 5). A431, H1650 and H3255 showed good tumor to lung (T/L) ratios. As shown in Fig. 6, there is a significant correlation between ^{125}I-PHY uptake and gefitinib sensitivity (IC_{50}) ($r=-0.900$, $p<0.05$).

DISCUSSION

We investigated the correlation between *in vivo* tumor uptake of ^{125}I-PHY and gefitinib sensitivity. In this study, we used one epidermoid carcinoma cell line and four NSCLC cell lines with different levels of EGFR expression and mutation status. These cell lines showed a range of gefitinib sensitivities. The present study indicated that the radioiodinated PHY is able to estimate gefitinib sensitivity based on EGFR expression levels.

Biodistribution studies indicated that ^{125}I-PHY is significantly taken up in the intestine, followed by the stomach and liver. This biodistribution was similar to that of other EGFR-TK imaging agents.[14,19] One preferable characteristic is that ^{125}I-PHY uptake in blood, lung and brain is low, resulting in relatively high T/B and T/L ratios. This suggests that radioiodinated PHY is useful for imaging lung and brain tumors.

The *in vivo* tumor uptake of ^{125}I-PHY is EGFR-TK specific and is negatively correlated with the IC_{50} values of gefitinib in five cell lines. These results are in accordance with the previ-

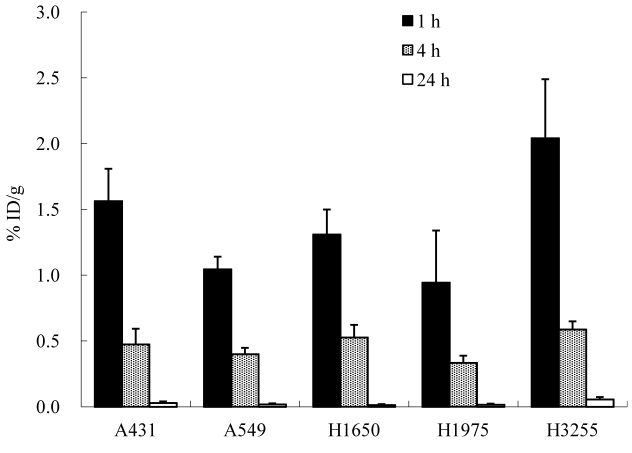

Fig. 4. *In Vivo* Uptake of ^{125}I-PHY in Tumor Bearing Mice ($n=4$)

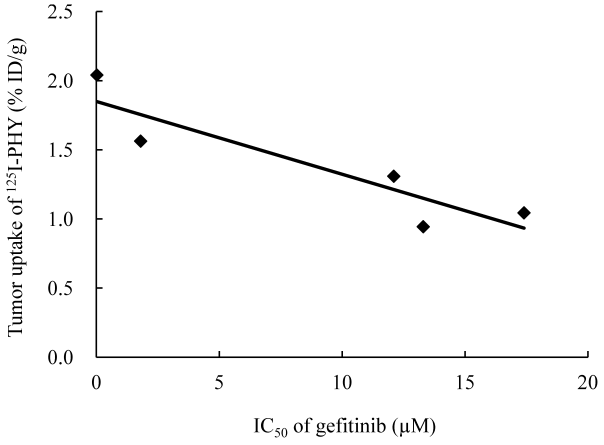

Fig. 6. Correlation between *in Vivo* Tumor Uptake at 1 h and Gefitinib Sensitivity ($r=-0.900$, $p<0.05$)

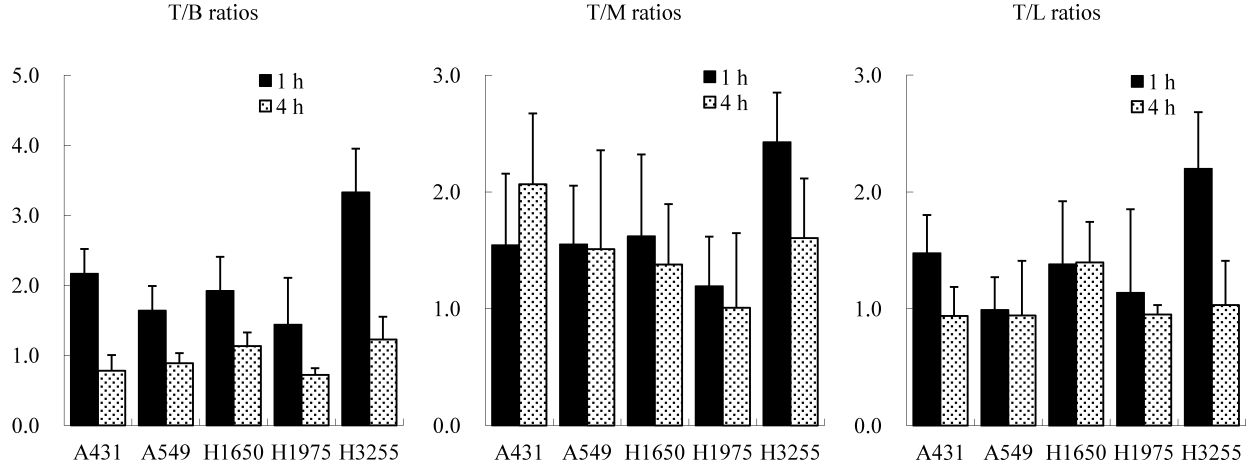

Fig. 5. Tumor to Blood (T/B), Muscle (T/M) and Lung (T/L) Ratios of ^{125}I-PHY

ous results[18] that indicate correlations between ^{11}C-PD153035 uptake and EGFR expression levels, as measured by flow cytometry. PHY is structurally similar to PD153035 and the inhibitory potency of PHY against EGFR-TK phosphorylation is the same as that of PD153035.

Some tumor uptake is caused by nonspecific binding of ^{125}I-PHY, most likely to the cell membrane. In A431 and A549 harboring wild-type EGFR, gefitinib sensitivity of A431 was 10-fold higher than that of A549 and western blotting also showed abundant expression of EGFR in A431 when compared with A549, while ^{125}I-PHY uptake in A431 was only 1.5-fold higher than that in A549. An excess of gefitinib reduced ^{125}I-PHY uptake in A431 up to 52%. Therefore, reduction in nonspecific binding would result in estimating EGFR expression in more detail.

Although radiolabeled gefitinib should be suitable for estimating gefitinib sensitivity and assessing mutation status, ^{18}F-gefitinib did not reflect EGFR expression levels.[14] ^{125}I-PHY and ^{11}C-PD153035 were washed out of tumors, whereas ^{18}F-gefitinib was retained in tumors throughout the experiment. These observations suggest that nonspecific binding of ^{18}F-gefitinib to the cell membrane predominantly contributes to tumor uptake. In comparison with gefitinib, therefore, PHY and PD153035 may successfully penetrate into the cell membrane and then bind to EGFR-TK.

Estimation of EGFR expression would be a useful index for selecting patients to benefit from treatment with EGFR-TK inhibitors and to monitor inhibition status. Several groups[9–11] have shown that mutations in the TK domain of the EGFR gene are significantly correlated with clinical response to gefitinib therapy. Therefore, this mutation is a candidate to predict gefitinib sensitivity. Unfortunately, there are no significant differences in tumor uptake and clearance of ^{125}I-PHY between cells with wild-type EGFR and mutant EGFR. However, the overexpression is a prerequisite for treatment with EGFR-TK inhibitors.

Imaging agents are required to detect mutation status for accurate prediction of therapeutic efficacy with EGFR-TK inhibitors. The level of EGFR expression in tumors is, in itself, insufficient to account for their sensitivity to treatment.[22,23] PHY and PD153035 showed slight enhancement of growth inhibition in H3255, with the IC_{50} values for PHY and PD153035 being 3.1- and 5.6-fold lower than those in A431, respectively. In contrast, gefitinib showed marked growth inhibition in H3255, in which the IC_{50} of gefitinib is 90-fold lower than in A431. Crystal structure analysis[24,25] revealed that substitution of Leu858 with arginine maintains kinase activity in the active state and allows gefitinib to move deeper inside the binding pocket. Although ^{18}F-gefitinib is unsuitable for imaging EGFR-TK activity, these findings suggest that introduction of propylmorpholino or other substituents to the 6 position of quinazoline is required for assessing mutation status.

CONCLUSION

Although EGFR expression levels are not sufficient to predict treatment efficacy with EGFR-TK inhibitors, EGFR overexpression in tumors is an essential factor for EGFR targeted therapy. Our study suggested that radioiodinated PHY is a potential imaging agent to detect EGFR expression levels as a first screening marker and we require further modifications of the compound to accurately estimate gefitinib sensitivity.

Acknowledgments This work was supported by Grants-in-Aid for Scientific Research (C) No.10770466, No.19591437, (B) No.18390331 from JSPS and a Grant-in-Aid for High Technology Research from the Ministry of Education, Culture, Sports, Science and Technology of Japan.

REFERENCES

1) Salomon DS, Brandt R, Ciardiello F, Normanno N. Epidermal growth factor-related peptides and their receptors in human malignancies. *Crit. Rev. Oncol. Hematol.*, **19**, 183–232 (1995).
2) Laskin JJ, Sandler AB. Epidermal growth factor receptor: a promising target in solid tumours. *Cancer Treat. Rev.*, **30**, 1–17 (2004).
3) Yarden Y, Sliwkowski MX. Untangling the ErbB signalling network. *Nat. Rev. Mol. Cell Biol.*, **2**, 127–137 (2001).
4) Marshall J. Clinical implications of the mechanism of epidermal growth factor receptor inhibitors. *Cancer*, **107**, 1207–1218 (2006).
5) Fukuoka M, Yano S, Giaccone G, Tamura T, Nakagawa K, Douillard JY, Nishiwaki Y, Vansteenkiste J, Kudoh S, Rischin D, Eek R, Horai T, Noda K, Takata I, Smit E, Averbuch S, Macleod A, Feyereislova A, Dong RP, Baselga J. Multi-institutional randomized phase II trial of gefitinib for previously treated patients with advanced non-small-cell lung cancer (The IDEAL 1 Trial). *J. Clin. Oncol.*, **21**, 2237–2246 (2003).
6) Kris MG, Natale RB, Herbst RS, Lynch TJ Jr, Prager D, Belani CP, Schiller JH, Kelly K, Spiridonidis H, Sandler A, Albain KS, Cella D, Wolf MK, Averbuch SD, Ochs JJ, Kay AC. Efficacy of gefitinib, an inhibitor of the epidermal growth factor receptor tyrosine kinase, in symptomatic patients with non-small cell lung cancer: a randomized trial. *JAMA*, 290, 2149–2158 (2003).
7) Inoue A, Saijo Y, Maemondo M, Gomi K, Tokue Y, Kimura Y, Ebina M, Kikuchi T, Moriya T, Nukiwa T. Severe acute interstitial pneumonia and gefitinib. *Lancet*, **361**, 137–139 (2003).
8) Jänne PA, Engelman JA, Johnson BE. Epidermal growth factor receptor mutations in non-small-cell lung cancer: implications for treatment and tumor biology. *J. Clin. Oncol.*, **23**, 3227–3234 (2005).
9) Paez JG, Janne PA, Lee JC, Tracy S, Greulich H, Gabriel S, Herman P, Kaye FJ, Lindeman N, Boggon TJ, Naoki K, Sasaki H, Fujii Y, Eck MJ, Sellers WR, Johnson BE, Meyerson M. EGFR mutations in lung cancer: correlation with clinical response to gefitinib therapy. *Science*, **304**, 1497–1500 (2004).
10) Lynch TJ, Bell DW, Sordella R, Gurubhagavatula S, Okimoto RA, Brannigan BW, Harris PL, Haserlat SM, Supko JG, Haluska FG, Louis DN, Christiani DC, Settleman J, Haber DA. Activating mutations in the epidermal growth factor receptor underlying responsiveness of non-small-cell lung cancer to gefitinib. *N. Engl. J. Med.*, **350**, 2129–2139 (2004).
11) Giaccone G, Rodriguez JA. EGFR inhibitors: what have we learned from the treatment of lung cancer? *Nat. Clin. Pract. Oncol.*, **2**, 554–561 (2005).
12) Thakur ML. Genomic biomarkers for molecular imaging: predicting the future. *Semin. Nucl. Med.*, **39**, 236–246 (2009).
13) Chen X, Park R, Shahinian AH, Bading JR, Conti PS. Pharmacokinetics and tumor retention of ^{125}I-labeled RGD peptide are improved by PEGylation. *Nucl. Med. Biol.*, **31**, 11–19 (2004).
14) Su H, Seimbille Y, Ferl GZ, Bodenstein C, Fueger B, Kim KJ, Hsu YT, Dubinett SM, Phelps ME, Czernin J, Weber WA. Evaluation of [^{18}F]gefitinib as a molecular imaging probe for the assessment of the epidermal growth factor receptor status in malignant tumors. *Eur. J. Nucl. Med. Mol. Imaging*, **35**, 1089–1099 (2008).
15) Mishani E, Abourbeh G, Jacobson O, Dissoki S, Ben Daniel R, Rozen Y, Shaul M, Levitzki A. High-affinity epidermal growth factor receptor (EGFR) irreversible inhibitors with diminished chemi-

cal reactivities as positron emission tomography (PET)-imaging agent candidates of EGFR overexpressing tumors. *J. Med. Chem.*, **48**, 5337–5348 (2005).

16) Ortu G, Ben-David I, Rozen Y, Freedman NM, Chisin R, Levitzki A, Mishani E. Labeled EGFr-TK irreversible inhibitor (ML03): *in vitro* and *in vivo* properties, potential as PET biomarker for cancer and feasibility as anticancer drug. *Int. J. Cancer*, **101**, 360–370 (2002).
17) Pal A, Glekas A, Doubrovin M, Balatoni J, Namavari M, Beresten T, Maxwell D, Soghomonyan S, Shavrin A, Ageyeva L, Finn R, Larson SM, Bornmann W, Gelovani JG. Molecular imaging of EGFR kinase activity in tumors with ^{124}I-labeled small molecular tracer and positron emission tomography. *Mol. Imaging Biol.*, **8**, 262–277 (2006).
18) Wang H, Yu J, Yang G, Song X, Sun X, Zhao S, Mu D. Assessment of ^{11}C-labeled-4-*N*-(3-bromoanilino)-6,7-dimethoxyquinazoline as a positron emission tomography agent to monitor epidermal growth factor receptor expression. *Cancer Sci.*, **98**, 1413–1416 (2007).
19) Abourbeh G, Dissoki S, Jacobson O, Litchi A, Ben Daniel R, Laki D, Levitzki A, Mishani E. Evaluation of radiolabeled ML04, a putative irreversible inhibitor of epidermal growth factor receptor, as a bioprobe for PET imaging of EGFR-overexpressing tumors. *Nucl. Med. Biol.*, **34**, 55–70 (2007).
20) Mishani E, Hagooly A. Strategies for molecular imaging of epidermal growth factor receptor tyrosine kinase in cancer. *J. Nucl. Med.*, **50**, 1199–1202 (2009).
21) Hirata M, Kanai Y, Naka S, Matsumuro K, Kagawa S, Yoshimoto M, Ohmomo Y. Synthesis and evaluation of radioiodinated phenoxyquinazoline and benzylaminoquinazoline derivatives as new EGF receptor tyrosine kinase imaging ligands for tumor diagnosis using SPECT. *Ann. Nucl. Med.*, **26**, 381–389 (2012).
22) Suzuki T, Nakagawa T, Endo H, Mitsudomi T, Masuda A, Yatabe Y, Sugiura T, Takahashi T, Hida T. The sensitivity of lung cancer cell lines to the EGFR-selective tyrosine kinase inhibitor ZD1839 ('Iressa') is not related to the expression of EGFR or HER-2 or to K-ras gene status. *Lung Cancer*, **42**, 35–41 (2003).
23) Helfrich BA, Raben D, Varella-Garcia M, Gustafson D, Chan DC, Bemis L, Coldren C, Baron A, Zeng C, Franklin WA, Hirsch FR, Gazdar A, Minna J, Bunn PA Jr. Antitumor activity of the epidermal growth factor receptor (EGFR) tyrosine kinase inhibitor gefitinib (ZD1839, Iressa) in non-small cell lung cancer cell lines correlates with gene copy number and EGFR mutations but not EGFR protein levels. *Clin. Cancer Res.*, **12**, 7117–7125 (2006).
24) Yun CH, Boggon TJ, Li Y, Woo MS, Greulich H, Meyerson M, Eck MJ. Structures of lung cancer-derived EGFR mutants and inhibitor complexes: mechanism of activation and insights into differential inhibitor sensitivity. *Cancer Cell*, **11**, 217–227 (2007).
25) Liu B, Bernard B, Wu JH. Impact of EGFR point mutations on the sensitivity to gefitinib: insights from comparative structural analyses and molecular dynamics simulations. *Proteins*, **65**, 331–346 (2006).